MOLECULAR AND CELLULAR BIOLOGY, Jan. 2009, p. 378–388 Vol. 29, No. 2
0270-7306/09/$08.00+0 doi:10.1128/MCB.01661-08

Deletion of Shp2 Tyrosine Phosphatase in Muscle Leads to Dilated Cardiomyopathy, Insulin Resistance, and Premature Death[▽]

Frederic Princen,[1] Emilie Bard,[1] Farah Sheikh,[2] Sharon S. Zhang,[1] Jing Wang,[1] Wagner M. Zago,[1] Dongmei Wu,[1] Ramon Diaz Trelles,[1] Beatrice Bailly-Maitre,[1] C. Ronald Kahn,[4] Yan Chen,[5] John C. Reed,[1] Gary G. Tong,[1,3] Mark Mercola,[1] Ju Chen,[2] and Gen-Sheng Feng[1,6]*

Burnham Institute for Medical Research, 10901 N. Torrey Pines Road, La Jolla, California 92037[1]; Department of Medicine, University of California San Diego, La Jolla, California 92093[2]; Department of Neurosciences, University of California, San Diego, La Jolla, California 92093[3]; Research Division, Joslin Diabetes Center, Harvard Medical School, Boston, Massachusetts 02215[4]; Institute for Nutritional Sciences, Chinese Academy of Sciences, Shanghai 200031, China[5]; and Institute for Biomedical Research, Xiamen University, Xiamen 361005, China[6]

Received 24 October 2008/Accepted 27 October 2008

The intracellular signaling mechanisms underlying the pathogenesis of cardiac diseases are not fully understood. We report here that selective deletion of Shp2, an SH2-containing cytoplasmic tyrosine phosphatase, in striated muscle results in severe dilated cardiomyopathy in mice, leading to heart failure and premature mortality. Development of cardiomyopathy in this mouse model is coupled with insulin resistance, glucose intolerance, and impaired glucose uptake in striated muscle cells. Shp2 deficiency leads to upregulation of leukemia inhibitory factor-stimulated phosphatidylinositol 3-kinase/Akt, Erk5, and Stat3 pathways in cardiomyocytes. Insulin resistance and impaired glucose uptake in Shp2-deficient mice are at least in part due to impaired protein kinase C-ζ/λ and AMP-kinase activities in striated muscle. Thus, we have generated a mouse line modeling human patients suffering from cardiomyopathy and insulin resistance. This study reinforces a concept that a compound disease with multiple cardiovascular and metabolic disturbances can be caused by a defect in a single molecule such as Shp2, which modulates multiple signaling pathways initiated by cytokines and hormones.

Heart failure is a serious life-threatening health problem worldwide. Numerous studies have demonstrated a link between cardiac dysfunction and insulin resistance, as well as deficiency in glucose transport (9, 35, 48). In the absence of manifest diabetes, insulin resistance and minor degrees of glucose intolerance are thought to be associated with and contribute to the development of nonischemic cardiomyopathy or idiopathic dilated cardiomyopathy (35, 45). However, the molecular basis for this link is poorly understood.

Muscle-specific gene knockout mice have presented unprecedented opportunities to decipher molecular signaling mechanisms underlying cardiomyopathic changes. Deletion of PTEN in cardiomyocytes mediated by Mck-Cre results in cardiac hypertrophy in mice (8). Dilated cardiomyopathy was also observed to various degrees in mice with conditional ablation of ErbB2 (HER2), β_1 integrin, and the gp130 cytokine receptor component in the heart or muscle (16, 34, 37). Interestingly, despite the development of cardiomyopathy, most of these mutant mice survive to adulthood with a normal life span, suggesting limitations in their modeling of human patients' pathological processes. These mutant mouse models also show no correlation between cardiomyopathy and insulin resistance. In fact, although muscle-specific PTEN knockout mice develop cardiac hypertrophy (8), they are protected against insulin resistance and diabetes induced by high-fat diet due to enhanced insulin-stimulated glucose uptake in soleus muscle (43).

Shp2 is a widely expressed cytoplasmic tyrosine phosphatase with two SH2 domains that has been implicated in signaling events downstream of receptors for growth factors, cytokines, and hormones (25, 32). In particular, Shp2 has been shown to participate in leptin and insulin signaling for the regulation of energy balance and metabolism (23, 28, 46). In recent experiments, several groups have identified germ line gain and loss-of-function mutations in the human gene *PTPN11*, encoding Shp2, in Noonan syndrome and LEOPARD (for lentigines, electrocardiogram abnormalities, ocular hypertelorism, pulmonic valvular stenosis, abnormalities of genitalia, retardation of growth, and deafness) syndrome patients, respectively (21, 42). Paradoxically, these mutations either constitutively activate or inactivate the phosphatase activity leading to heart diseases, among other disorders observed in Noonan or LEOPARD syndrome patients. Since the conventional Shp2 knockout mice are embryonic lethal (36), tissue-specific deletion of Shp2 will be required to determine a specific function for Shp2 in the cardiovascular system in vivo.

We report here that striated muscle-specific Shp2 knockout (MSKO) mice develop a severe dilated cardiomyopathy, resulting in heart failure and premature death in mice. More importantly, development of cardiomyopathy is associated with insulin resistance, glucose intolerance, and impaired insulin-stimulated glucose uptake in striated muscle cells in this mouse model.

* Corresponding author. Mailing address: Burnham Institute for Medical Research, 10901 N. Torrey Pines Rd., La Jolla, CA 92037. Phone: (858) 795-5265. Fax: (858) 713-6274. E-mail: gfeng@burnham.org.

▽ Published ahead of print on 10 November 2008.

MATERIALS AND METHODS

Generation of MSKO mice. The *Shp2* floxed allele and *Mck-Cre* mice have been described previously (3, 46). *Shp2*$^{flox/flox}$ mice were used as controls, *Shp2*$^{flox/+}$; *Mck-Cre*/+ mice were used as a heterozygous mutant, and *Shp2*$^{flox/flox}$; *Mck-Cre*/+ mice were used as homozygous mutant (MSKO). Mice were bred and maintained according to the standard animal facility procedures. Deletion of *Shp2* exon4 was determined as previously described (46). Unless indicated, data were collected from experiments on male animals.

Immunoblotting, immunoprecipitation, and kinase assay. Human insulin (5 U; Lilly) or mouse Leukemia Inhibitory Factor (LIF; 6×10^4 U/kg; Esgro) was injected into the inferior vena cavas of 4- to 5-week-old mice. Whole-cell protein extracts were isolated from the heart, muscle, and liver of each animal. Immunoprecipitation and immunoblot studies were performed according to standard protocols. The rabbit polyclonal antibodies against phospho-Akt (Thr308 or Ser473), Akt, phospho-AMP-kinase (phospho-AMPK), AMPK, phospho-Erk5, Erk5 phospho-Erk1/2, Erk1/2, phospho-Jnk1/2, Jnk1/2, phospho-p90RSK, p90rsk, phospho-p70^{s6k}, p70^{s6k}, phospho-protein kinase C (PKC)-ζ/λ, and PKC-ζ/λ were obtained from Cell Signaling. Rabbit polyclonal anti-Shp2 antibody was generated in this laboratory, mouse α-tubulin was obtained from Sigma, and rabbit polyclonal GLUT4 was purchased at Chemicon. The Akt kinase assay was performed as directed by Cell Signaling.

qRT-PCR. Total RNA was isolated by using the RNA STAT-60 reagent protocol (Tel-Test). Quantitative reverse transcription-PCR (qRT-PCR) experiments were carried out according to a one-step Sybr green qRT-PCR kit protocol (Stratagene) using an MX3000P thermal cycler (Stratagene). The primer sequences used were 5′-TTGGAGCAAATCCTGTGTAC-3′ and 5′-CTTCCTC AGTCTGCTCACTC-3′ for atrial natriuretic factor (ANF), 5′-AAGAGTCCT TCGGTCTCAAG-3′ and 5′-CCAGGAGGTCTTCCTACACC-3′ for b-type natriuretic peptide (BNP), 5′-TGCCAACAATGTCCTATCT-3′ and 5′-CTGCCT CATCATACTCTTG-3′ for skeletal α-actin, 5′-AACCTGGGAACAGAAAAC TG-3′ and 5′-GGCAAAAGTAGGGAGACAAG-3′ for phospholamban (PLN), 5′-AGTCTTAACGGCAGTGTGAG3′ and 5′-GTTGCTAACAACGCACAT G-3′ for sarcoendoplasmic reticulum Ca^{2+}-ATPase (SERCA2a), and 5′-GGTG CTGACGGGAACAAC-3′ and 5′-CAGTTTTCAATGCTTTTGTTGG-3′ for MEF2C. Each reaction was done in triplicate, and the expression data were normalized against GAPDH (glyceraldehyde-3-phosphate dehydrogenase).

Echocardiography analysis. Mice were anesthetized with isofluorane and subjected to echocardiography as previously described (41).

Primary cardiomyocyte culture. For neonatal primary cardiomyocyte cultures, 1-day-old neonatal mice were used. Hearts were removed aseptically and maintained in Dulbecco modified Eagle medium–F-12 medium (DMEM/F12). The cells were dissociated at 37°C by trypsin digestion 0.25% (wt/vol) (Sigma). The digestion mixture was filtered by using a 70-μm-pore-size nylon cell strainer (BD Falcon) and centrifuged for 10 min at 1,000 rpm, and cells were resuspended in DMEM/F12 with 20% fetal bovine serum. To exclude noncardiomyocytic cells, the cell suspension was preplated at 37°C for 1 h on plastic dishes. The remaining cells in the supernatant were then plated on collagen-coated dishes.

Electrophysiology. Electrophysiological patch clamp recordings were performed using conventional whole-cell configuration from neonatal primary cardiomyocytes, approximately 24 to 48 h after plating. I_{Ca} activation was measured by 40-ms test pulses to a series of potentials (−40 mV to +60 mV at 10-mV increments) applied at 10-s intervals from a holding potential of −50 mV. The capacitative currents evoked by the voltage jump were isolated with 2 mM extracellular cobalt (Co^{2+}) and subtracted from the recorded calcium currents. Total cell membrane capacitance was determined by integration of current transients in response to 10-mV test pulses. Calcium current density was used to minimize the effects of cell size on calcium currents. Patch pipettes were pulled to resistances of 2 to 3 MΩ. The data were analyzed on an IBM-compatible computer interfaced to an Axopatch (200B) amplifier (Axon Instruments) under the control of pCLAMP (version 8.0; Axon Instruments, Fremont, CA). The voltage dependence of calcium current activation was determined by using an interactive nonlinear regression-fitting procedure to the Boltzmann equation. Graphics and statistical data analysis were performed by using Prism (GraphPad Software, San Diego, CA).

Physiological assays. Blood glucose levels were assessed on whole venous blood using a One Touch Basic (Lifescan) glucose monitor. Serum insulin levels were measured by using the rat insulin enzyme-linked immunosorbent assay kit (Crystal Chem). Glucose tolerance tests were performed on overnight (13 to 15 h)-fasted mice by intraperitoneal injection of D-glucose (2 g/kg [body weight]; Sigma). Insulin resistance was tested on randomly fed mice after intraperitoneal injection of human insulin (1 U/kg [body weight]; Lilly). The serum-free fatty acids were measured by using the NEFA C test kit (Wako). Serum triglycerides were quantified using the triglyceride reagent set (Pointe Scientific, Inc).

Glucose uptake assays. Neonatal primary cardiomyocytes were used to measure glucose uptake, following published protocols (5, 11). Cells were plated in DMEM/F12 at 10^5 cells/96 wells. After 48 h, the medium was removed, and cells were washed with Krebs-Ringer phosphate-HEPES (KRPH) buffer and subsequently incubated with KRPH buffer at 37°C for 3 h. Insulin was added at various concentrations in KRPH buffer for 30 min at 37°C. Cells were then incubated with 0.2 μCi of 2-deoxy-D-[U-^{14}C]glucose (Amersham Biosciences) plus 100 μM cold 2-deoxy-D-glucose (Sigma-Aldrich) for 3 h at 37°C. The cells were washed with cold phosphate-buffered saline. For skeletal muscle, soleus muscles strips were used to monitor glucose uptake according to a previously published protocol (44).

Statistical analysis. Statistical analyses were done by using the Student unpaired *t* test. A *P* value of <0.05 was considered statistically significant. The data are presented as means ± the standard errors of the mean. Survival curves were determined according to the Kaplan-Meier survival analysis.

RESULTS

Generation of MSKO Shp2 mice. In previous studies, we generated a conditional *Shp2* mutant allele (*Shp2*^{flox}) in mice using the Cre-loxP technology (46), which allows for cell-type-specific Shp2 ablation. We generated a mouse strain with *Shp2* selectively deleted in striated muscle by crossing *Shp2*$^{flox/flox}$ mice with *Mck-Cre* transgenic animals that express the Cre recombinase under the control of the muscle creatine kinase promoter (Mck) (3). PCR analysis showed that Shp2 deletion occurred selectively in cardiac and skeletal muscle, with no DNA recombination events detected in other tissue/organs, such as the liver, lung, spleen, and kidney (Fig. 1A). Shp2 protein was also dramatically reduced in cardiac and skeletal muscles compared to controls (Fig. 1B), and the remaining faint bands in muscle samples are likely due to Shp2 expression in nonmyocytes such as fibroblast and endothelial cells. Shp2 ablation did not lead to increase in muscle expression levels of Shp1, which is predominantly expressed in hematopoietic cells (Fig. 1B). No obvious phenotypic differences were observed between control (*Shp2*$^{flox/flox}$) and heterozygous (*Shp2*$^{flox/+}$; *Mck-Cre*/+) mice, and thus most of the experiments were performed by comparing control (*Shp2*$^{flox/flox}$) and MSKO (*Shp2*$^{flox/flox}$; *Mck-Cre*/+) male mice. Immunostaining of control cardiomyocytes revealed that Shp2 expression was primarily localized to the T-tubular networks, while this expression was not detected in MSKO cardiomyocytes (Fig. 1C).

MSKO mice exhibit early postnatal lethality and develop dilated cardiomyopathy. Selective deletion of Shp2 in striated muscle did not affect the Mendelian frequency of MSKO male and female mice at birth. MSKO pups were viable up to 1 week after birth, with no obvious phenotypic differences compared to control littermates. However, MSKO mice began to die within 2 weeks after birth (Fig. 1D). In contrast, the survival of *Shp2*$^{flox/fox}$ control mice was 100%, as expected. The median survival age for the mutant mice is 13.4 weeks, with very few mice living up to 36 weeks. Between 5 and 9 weeks, no significant changes in body weights were observed between MSKO and control mice (Fig. 1E). However, overall heart size was significantly increased in MSKO mice compared to controls (Fig. 1G). This was also reflected by the significant 66% increase in heart/body weight ratios in MSKO mice relative to controls (Fig. 1F).

Hematoxylin and eosin staining of MSKO hearts revealed enlarged right and left ventricular chambers with thinner walls

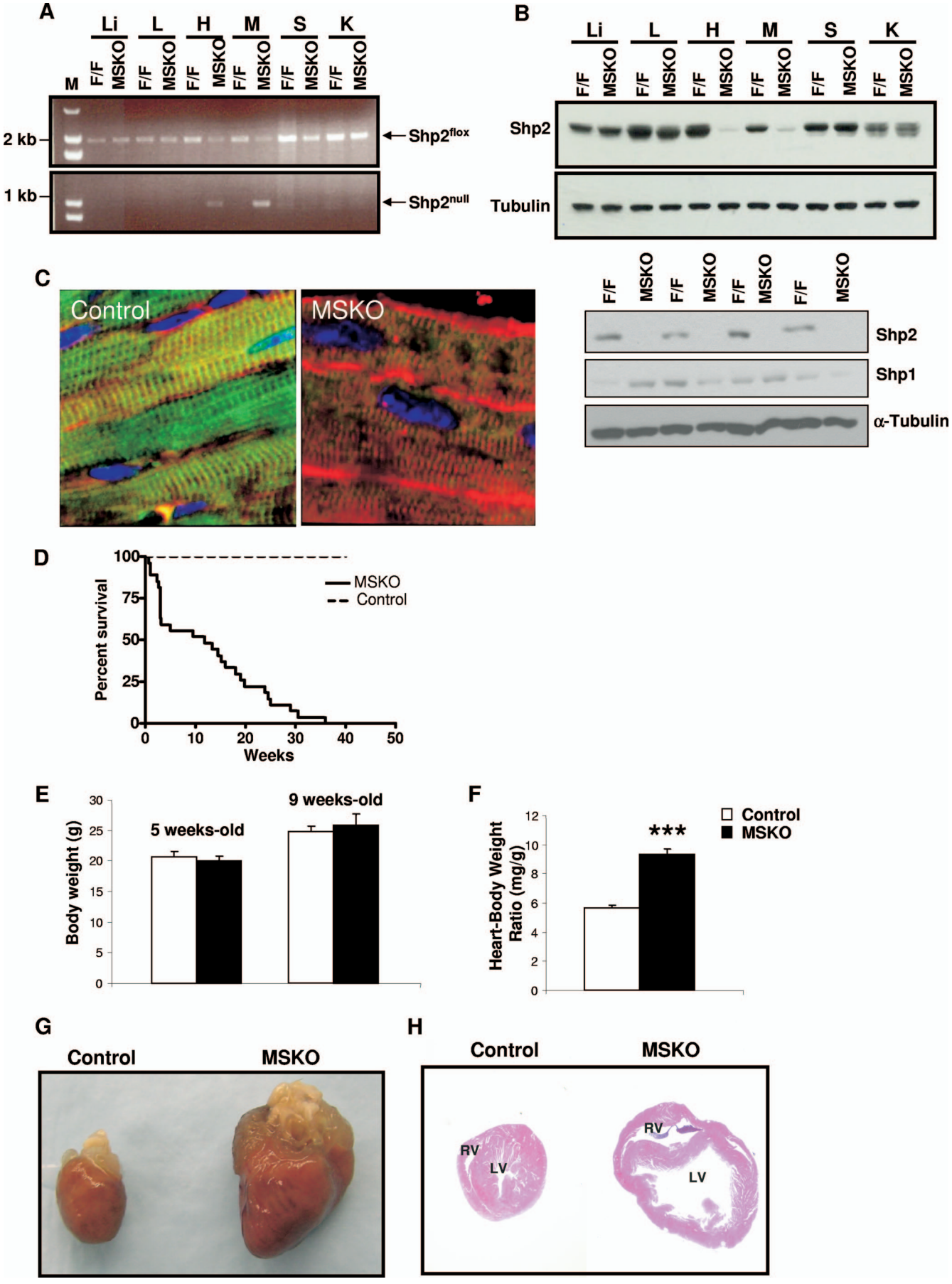

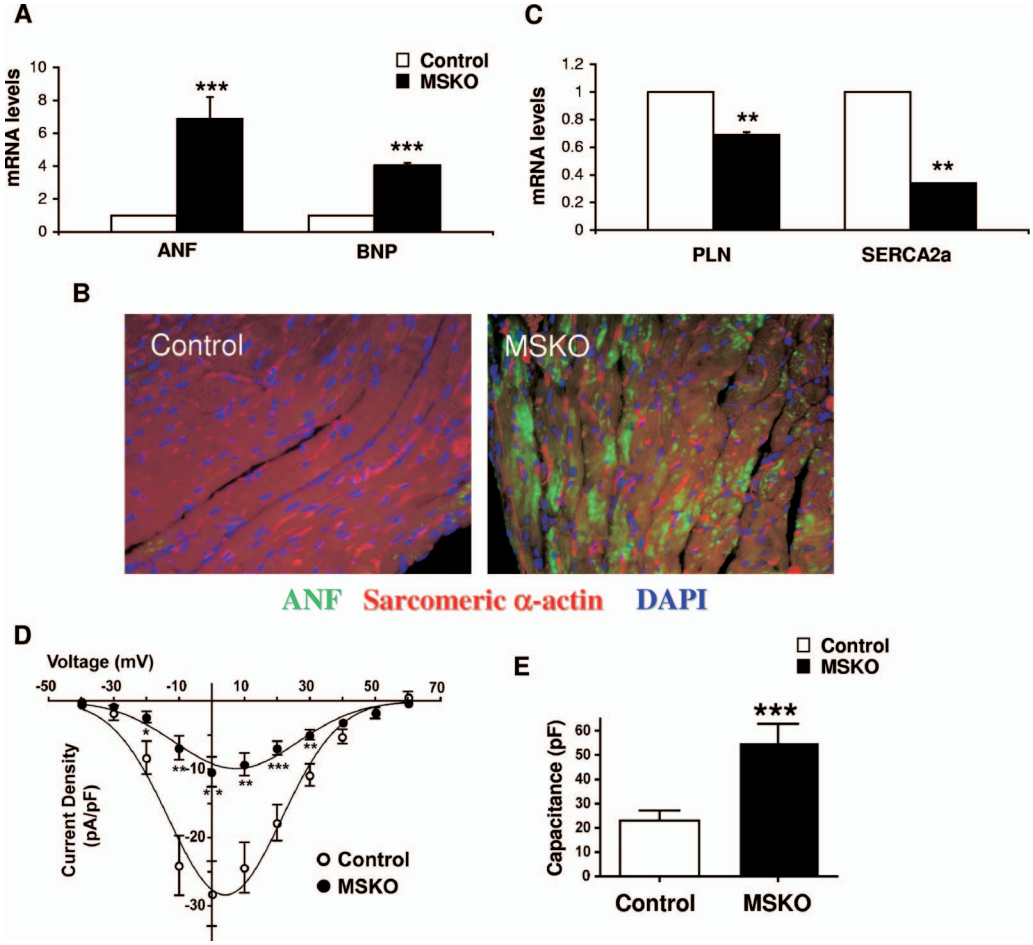

FIG. 2. Analysis of cardiac gene expression profile and calcium currents in male MSKO mice. (A) qPCR was performed on total RNA extracted from 4- to 5-week-old control (□) and MSKO (■) heart tissue. mRNA levels of ANF and BNP normalized against GAPDH are shown ($n = 3$). (B) Immunofluorescence staining of cardiac left ventricular sections with anti-ANF (green) and anti-sarcomeric α-actin (red) and DAPI (blue) (magnification, ×60). (C) qPCR analysis of mRNA levels of PLN and SERCA2a ($n = 3$). (D) L-type Ca^{2+} channel currents (I_{Ca}) measurement in postnatal primary cardiomyocyte derived from control (○) and MSKO (●) mice. Voltage-dependent changes in I_{Ca} in MSKO ($n = 13$) and control ($n = 14$) cells. I_{Ca} was normalized to the cell capacitance to yield current densities (pA/pF). (E) Cell capacitance (pF) of control ($n = 14$) and MSKO ($n = 13$) cardiomyocytes. *, $P < 0.05$; **, $P < 0.01$; ***, $P < 0.001$.

(Fig. 1H), which are common features of dilated cardiomyopathy. No significant abnormalities in liver, lung, and skeletal muscle could be detected in MSKO mice (data not shown). Masson's trichrome staining of MSKO hearts performed at different ages did not reveal evidence of fibrosis (data not shown). In addition, no significant changes in apoptosis or proliferation were detected in MSKO hearts compared to controls (data not shown). Furthermore, no significant difference in T-lymphocyte (CD4 and CD8) and macrophage (F4/80) marker staining was detected between MSKO and control hearts, suggesting a lack of lymphocyte and macrophage infiltration (data not shown).

To characterize cardiomyopathic changes in MSKO mice, we examined expression profiles of genes typically associated with cardiac stress (7, 17). mRNA levels of the *ANF* and *BNP* genes were assessed in 4- to 5-week-old control and mutant

FIG. 1. MSKO mice exhibit dilated cardiomyopathy. (A) PCR detection of Mck-Cre-mediated recombination event in DNA extracts from different tissues. Upper panel, $Shp2^{flox}$ allele; lower panel, $Shp2^{null}$ allele. M, molecular weight marker; Li, liver; L, lung; H, heart; M, skeletal muscle; S, spleen; K, kidney. (B) Immunoblot analysis of Shp2 protein expression in tissues from $Shp2^{flox/flox}$ (control) and MSKO mice. Shp1 expression was examined in skeletal muscles derived from control and MSKO mice with α-tubulin as a loading control (lower panels). (C) Immunofluorescence staining of cardiac left ventricular paraffin sections with antibodies to Shp2 (green) and anti-sarcomeric α-actin (red), as well as counterstained with DAPI (4′,6′-diamidino-2-phenylindole) (blue) (magnification, ×60). (D) Kaplan-Meier survival curves for control and MSKO mice ($n = 30$). (E) Body weight comparison between 5- and 9-week-old control mice (□) and MSKO mice (■) ($n = 20$). (F) Comparison of heart weight/body weight ratios between 5- and 9-week-old control and MSKO mice ($n = 13$). ***, $P < 0.001$. (G) Gross morphology of a representative heart from 12-week-old control and MSKO mice. (H) Transversal sections from 12 week-old control and MSKO mouse heart stained with hematoxylin and eosin. The right ventricle (RV) and left ventricle (LV) are shown. All experiments were done on male mice.

TABLE 1. In vivo echocardiographic assessment of cardiac size and function in control and MSKO (male) mice[a]

Parameter[b]	Mean ± SEM[c]	
	Control (n = 7)	MSKO (n = 7)
BW (g)	24 ± 0.8	25.4 ± 0.7
IVSd (mm)	0.60 ± 0.006	0.57 ± 0.01*
IVSs (mm)	1.01 ± 0.02	0.92 ± 0.04*
LVIDd (mm)	3.63 ± 0.08	4.54 ± 0.25*
LVIDs (mm)	2.04 ± 0.06	3.37 ± 0.27**
LVPWd (mm)	0.63 ± 0.01	0.59 ± 0.01
LVPWs (mm)	1.18 ± 0.03	1.09 ± 0.05
HR (bpm)	463 ± 35.4	454 ± 33.8
LV FS (%)	43.9 ± 1.4	26.4 ± 2.2**
VCF (circ/s)	8.09 ± 0.57	5.02 ± 0.49*
Ao-ET (ms)	55.4 ± 2.8	53.6 ± 2.9
Ao-HR (bpm)	463.9 ± 33.8	430.4 ± 30.6
LVMd (mg)	70.8 ± 3.4	97.6 ± 8.2*

[a] Echocardiographic measurements were obtained from transthoracic M-mode tracings of an average of 6-week-old mice.

[b] Abbreviations: BW, body weight; IVSd, interventricular septal wall thickness at end diastole; IVSs, interventricular septal wall thickness at end systole; LVIDd, left ventricular internal dimension at end diastole; LVIDs, left ventricular internal dimension at end systole; LVPWd, left ventricular posterior wall thickness at end diastole; LVPWs, left ventricular posterior wall thickness at end systole; HR, heart rate; LV FS, left ventricular fractional shortening; VCF, velocity of circumferential fiber shortening; Ao-ET, aortic ejection time; Ao-HR, aortic heart rate; LVMd, left ventricular mass at end diastole.

[c] *, $P < 0.05$; **, $P < 0.01$.

hearts. Notably, *ANF* and *BNP* expression was significantly elevated in MSKO mice (Fig. 2A and B). In contrast, *SERCA2a* expression was significantly downregulated in MSKO hearts by 56%, while a modest decrease in *PLN* expression was also observed in MSKO mice compared to controls (Fig. 2C). Both *SERCA2a* and *PLN* are known to be downregulated in heart failure and are involved in Ca^{2+} homeostasis, which plays a pivotal role in myocyte contractility. To detect alterations in L-type Ca^{2+} channel activities, we measured calcium currents (I_{Ca}) in cardiomyocytes by using the whole-cell patch clamp technique. MSKO cardiomyocytes exhibited significantly smaller I_{Ca} density (inward current amplitude normalized to cell capacitance, pA/pF) compared to controls (Fig. 2D). The current-voltage relationship was similar between both groups, suggesting that the channel properties were not altered (Fig. 2D). Conversely, cardiomyocyte capacitance, which is a measure of cell size, was significantly augmented in MSKO cardiomyocytes (Fig. 2E). Specifically, MSKO cells exhibited a twofold increase in capacitance compared to controls (control, 23 ± 4 pF, n = 14; MSKO, 55 ± 7 pF; n = 13) (Fig. 2E), a finding consistent with the altered expression profile of Ca^{2+} homeostasis genes and cardiac dysfunction observed. The decrease in I_{Ca} density in MSKO cardiomyocytes is likely a consequence of the increase in cell size not being accompanied by an increase in the expression of functional calcium channels.

Cardiac dysfunction in MSKO mice. The MSKO mice had significant abnormalities in cardiac dimensions and function, a finding suggestive of dilated cardiomyopathy. We then evaluated heart performance by using echocardiographic analysis (echo) in mutant and control male mice at an average age of 6 weeks (Table 1). Consistent with the histological analysis, MSKO mice had an enlarged left ventricular chamber size as evidenced by the significant increase in left ventricular internal dimension values at end diastole and end systole. In addition, significant wall thinning was seen in MSKO hearts, as evidenced by the significant decrease in systolic dimensions in interventricular septal wall thickness. However, no significant change in left ventricular posterior wall thickness was observed between MSKO and control mice. These changes in cardiac dimensions were accompanied by a striking decrease in cardiac function in mutant mice, as evidenced by the significant decrease in left ventricular fraction shortening and the velocity of circumferential fiber shortening. Echo analysis of left ventricular mass further confirmed the increase in heart size in MSKO mice.

Altered activation of PI3K/Akt pathway in hearts of MSKO mice. Alteration of the phosphatidylinositol 3-kinase (PI3K)/Akt pathway has been implicated in controlling cardiac size (4, 8, 27, 38). By direct immunoblot analysis, Akt phosphorylation on Ser473 and Thr308 was significantly increased in MSKO heart, compared to controls (Fig. 3A and C). Consistent with this observation, we detected increased phosphorylation of $p70^{s6k}$, a downstream target of Akt in MSKO hearts. Phosphorylation of GSK-3α/β on Ser21/9 residues, a substrate of Akt, was also increased in MSKO hearts compared to controls (Fig. 3B). However, no significant difference in Akt phosphorylation was observed in skeletal muscle of MSKO and control mice (Fig. 3C and D). These results suggest a unique negative role for Shp2 in modulating the PI3K/Akt pathway in cardiomyocytes.

Shp2 ablation leads to enhanced Erk5 and Stat3 activation by LIF in cardiomyocytes. LIF is a member of the interleukin-6 family of cytokines, which has been implicated in heart failure (18). We thus sought to examine the effects of LIF-induced cell signaling in Shp2-deficient cardiomyocytes. After LIF stimula-

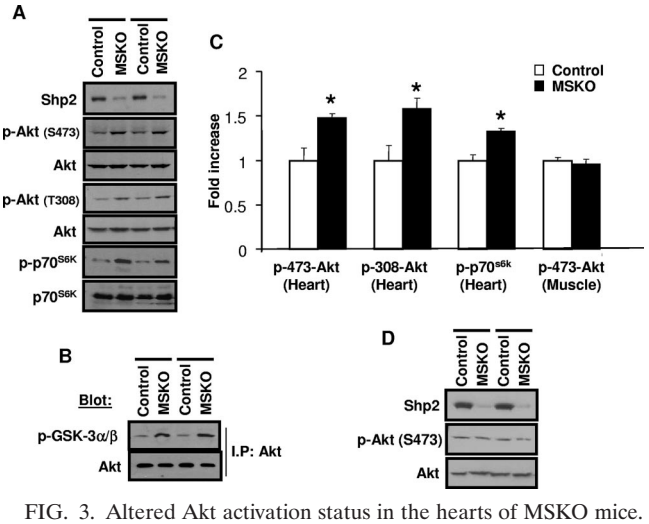

FIG. 3. Altered Akt activation status in the hearts of MSKO mice. (A) p-Akt (Ser473 and Thr308) and p-$p70^{s6k}$ phosphorylation were measured in 6- to 7-week-old heart lysates. (B) An Akt kinase assay was performed with immunoprecipitated Akt on GSK3 as a substrate, detected using anti-p-GSK3 α/β (Ser21/9). (C) Phosphoprotein levels of p-Akt and p-$p70^{s6k}$ were quantitated relative to the control protein amount (n = 3). *, $P < 0.05$. (D) p-Akt (Ser473) levels from 6- to 7-week-old skeletal muscle. All experiments were done on male animals.

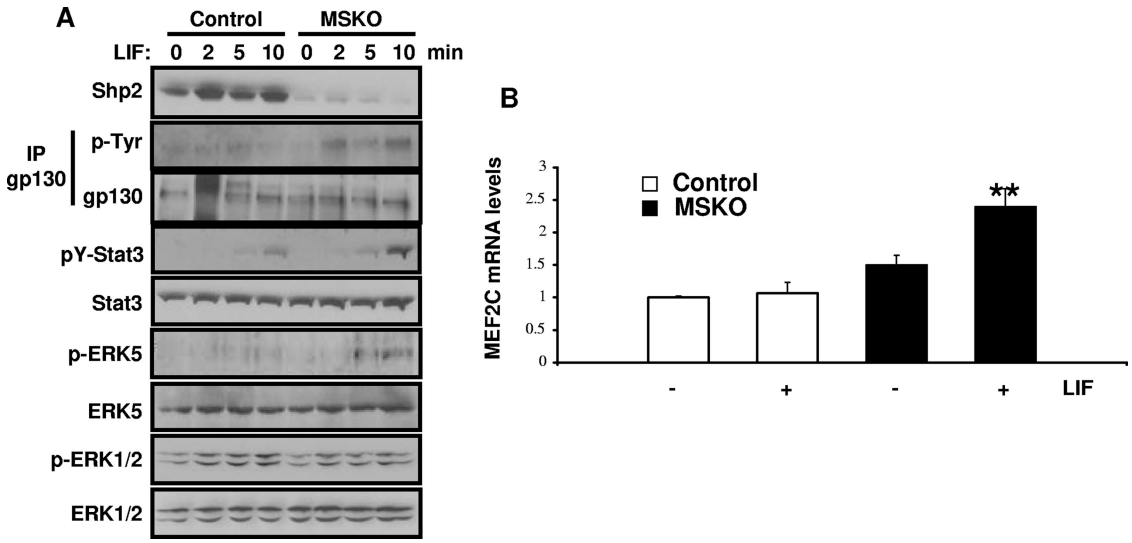

FIG. 4. Changes in LIF-mediated signaling in cardiomyocytes. (A) LIF (6×10^4 U/kg) was injected into the cava veins of overnight-fasted mice, and heart extracts were immunoblotted with antibodies as indicated. (B) qPCR analysis of *MEF2C* mRNA levels from 4- to 5-week-old hearts (normalized against *GAPDH*), with or without LIF stimulation (10 min) ($n = 3$). **, $P < 0.01$.

tion, Erk5 phosphorylation was upregulated in Shp2-deficient hearts, while phospho-Erk1/2 levels were decreased (Fig. 4A). To further confirm the enhanced Erk5 activation, we monitored *Mef2c* expression and found that LIF-induced *Mef2c* expression was increased in MSKO hearts compared to controls (Fig. 4B). In addition, LIF-induced tyrosine phosphorylation of Stat3, which is associated with increased gp130 tyrosine phosphorylation, was elevated in MSKO hearts compared to controls (Fig. 4A). This is consistent with our previous observation of a negative role for Shp2 in modulation of Stat3 activity (2, 46).

MSKO mice exhibit insulin resistance and glucose intolerance. The effects of Shp2 deficiency on glucose homeostasis and metabolism were assessed in MSKO mice. No significant differences in blood glucose levels were observed in the fed and fasted conditions between control and MSKO mice (Fig. 5A). However, circulating insulin levels under the fed and fasted conditions were slightly increased in sera of MSKO mice (Fig. 5B). As shown in Table 2, significantly elevated levels of triglycerides were observed in the plasma, hearts, and muscles of MSKO mice compared to controls. No increase in the amounts of circulating free fatty acids was observed in MSKO mice, and glycogen contents in cardiac and skeletal muscle in MSKO mice were comparable to those of controls.

We performed an insulin tolerance test on 6- to 7-week-old animals. Male and female MSKO mice displayed a remarkably decreased ability to lower circulating blood glucose levels after intraperitoneal injection of insulin (Fig. 5C). Consistent with impaired insulin sensitivity, we observed glucose intolerance in MSKO mice, with the most significant difference detected at 120 min after glucose injection (Fig. 5D). Therefore, MSKO mice developed insulin resistance in association with dilated cardiomyopathy.

Glucose uptake is impaired in Shp2-deficient cardiac and skeletal muscle cells. To determine the cellular basis of insulin resistance and glucose intolerance, we assessed the glucose uptake capacity of Shp2-deficient cardiac and skeletal muscle cells. Glucose transport was severely impaired in Shp2-deficient cardiomyocytes, with a >50% decrease in 2-deoxyglucose incorporation after 0.1 and 1 μM insulin stimulation (Fig. 6A). To determine glucose uptake in skeletal muscle, we isolated soleus muscle and performed an ex vivo glucose transport assay. As shown in Fig. 6B, glucose uptake was significantly impaired in MSKO skeletal muscle compared to controls. Therefore, Shp2 tyrosine phosphatase is required for insulin-stimulated glucose uptake in both cardiac and skeletal muscle cells.

To explore the molecular mechanism, we first examined tyrosine phosphorylation (pY) levels of the insulin receptor substrate-1 (IRS-1) protein. Surprisingly, insulin-induced pY-IRS1 signals were enhanced in heart and muscle lysates from MSKO mice compared to controls (Fig. 7A and B), with increased amounts of the p85-IRS1 complex detected by coimmunoprecipitation (Fig. 7A). Meanwhile, slightly lower levels of IRS-1 phosphorylation on Ser612 was detected in MSKO samples compared to controls (Fig. 7A and B). Notably, increased pY-IRS-1 signals were not detected in liver lysates of MSKO mice (Fig. 7C), in which Shp2 expression was not changed. These results suggest that insulin resistance induced by Shp2 deletion in muscle is not due to a defect at the level of IRS1. It is more likely that Shp2 deletion caused changes in other downstream signaling components, resulting in attenuated insulin signaling. We then examined activities of Akt and atypical PKC (PKC-ζ/λ) after insulin stimulation. In MSKO mice, PKC-ζ/λ activation was modestly decreased, with no dramatic change in Akt phosphorylation compared to controls (Fig. 7D). Muscle glucose transport is also regulated by a mechanism linked to the activation of AMPK. Metformin, a biguanide drug, is known to reduce insulin resistance and increase glucose uptake into peripheral tissues mainly by increasing AMPK activity (14, 47). AMPK activation by metformin

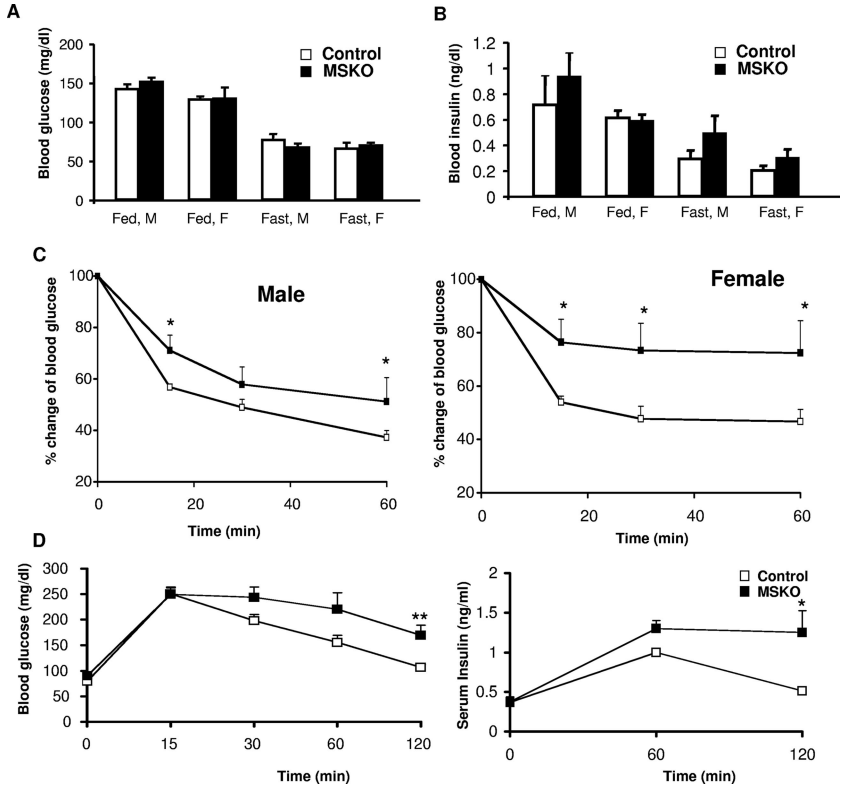

FIG. 5. Metabolic characterization of MSKO mice. (A) Blood glucose measured on randomly fed (fed) or 16-h-fasted (fast) male (M) and female (F) mice (n = 20 to 25). (B) Serum insulin levels were measured in fed and fasted mice (n = 7 to 10). (C) An insulin tolerance test was performed on 6- to 7-week-old male mice and on 6- to 8-week-old female mice (n = 7). (D) A glucose tolerance test was performed on 7- to 8-week-old 16-h-fasted male mice; n = 7. Serum insulin was measured during the glucose tolerance test. *, $P < 0.05$; **, $P < 0.01$.

was remarkably decreased in MSKO heart and skeletal muscle cells compared to controls (Fig. 7E).

Opposite effects of Shp2 on insulin-stimulated mitogen-activated protein kinase pathways. Consistent with the bidirectional effects of Shp2 in modulating Erk5 and Erk1/2 activation by LIF in cardiomyocytes, we observed similar bidirectional roles of Shp2 in the relay of insulin signaling. After insulin stimulation, phospho-Erk1/2 and phospho-Jnk1/2 levels were markedly decreased in Shp2-deficient cardiac and skeletal muscle tissues (Fig. 7F). Consistently, insulin-induced activation of $p90^{Rsk}$, a downstream target of Erk1/2, was downregulated in MSKO cardiac and skeletal muscle compared to controls (Fig. 7F). However, phospho-Erk5 signal was increased in cardiac and skeletal muscles of mutant mice.

TABLE 2. Metabolic changes in MSKO mice[a]

Parameter[b]	Mean ± SEM[c]			
	Male		Female	
	Control	MSKO	Control	MSKO
Fasted FFA (mmol/liter)	0.94 ± 0.03	0.98 ± 0.04	0.79 ± 0.04	0.83 ± 0.05
Fasted TG (mmol/liter)	1.08 ± 0.1	1.65 ± 0.29*	0.56 ± 0.03	1.0 ± 0.17*
Fasted muscle TG (mg/g)	1.79 ± 0.67	2.65 ± 0.89*	2.3 ± 0.6	4.7 ± 0.7*
Fasted heart TG (mg/g)	0.81 ± 0.08	1.09 ± 0.13*	0.79 ± 0.1	1.05 ± 0.08*
Fasted muscle glycogen (mg/g)	2.7 ± 0.2	2.5 ± 0.3	2.5 ± 0.2	2.7. ± 0.2
Fasted heart glycogen (mg/g)	4.5 ± 0.2	3.6 ± 0.2	4.9 ± 0.2	4.2. ± 0.4

[a] Mice were examined at the age of 5 to 6 weeks.
[b] Abbreviations: FFA, free fatty acids; TG, triglycerides.
[c] $n \geq 7$. *, $P < 0.05$.

DISCUSSION

In this study, we show that mice with a conditional deletion of Shp2 in muscle develop dilated cardiomyopathy and glucose intolerance, and die prematurely in early postnatal life. The development of dilated cardiomyopathy and heart failure in MSKO mice is corroborated by the increased expression of cardiac stress markers, such as ANF and BNP, in MSKO hearts compared to controls. Downregulation of SERCA2a was also observed in Shp2-deficient cardiomyocytes, and SERCA2a is a critical factor in regulation of cardiac Ca^{2+} homeostasis, with decreased expression detected during cardiac dysfunction (29). Echocardiographic analysis of MSKO hearts further demonstrated cardiac dysfunction coupled with ventricular chamber dilatation, characteristic of dilated cardiomyopathy. Molecular signaling analysis suggests that deletion of Shp2 leads to altered LIF-induced intracellular signals, including enhanced Stat3 and Erk5 activities, and impaired

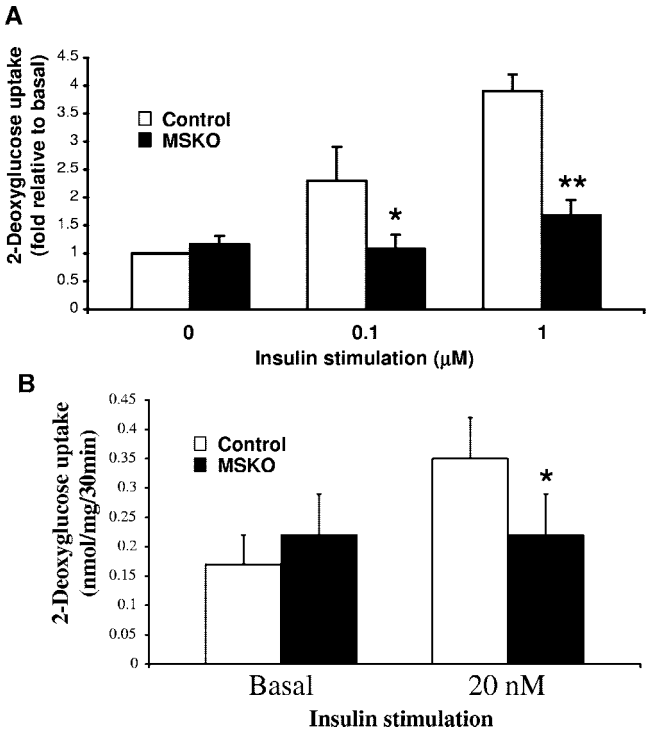

FIG. 6. Glucose uptake in cardiomyocytes and soleus muscle cells. (A) 2-Deoxyglucose uptake in neonatal primary cardiomyocytes. The uptake was determined at baseline and after 30 min of incubation with 0.1 or 1 μM insulin. (B) Soleus muscles were isolated, and glucose uptake was monitored ex vivo at baseline and after 30 min of incubation with 20 nM insulin ($n = 3$ to 5). *, $P < 0.05$; **, $P < 0.01$.

Erk1/2 activation. Consistently, Hagiwara et al. showed a putative role of Shp2 in mediating LIF-stimulated $[Ca^{2+}]_i$ transient and action potential duration increase in cardiomyocytes using knockin mice lacking a Shp2 docking site on gp130, a signal transducing component in LIF receptor (12). Heart-specific overexpression of Stat3 induced myocardial hypertrophy in mice, with elevated expression of ANF, β-myosin heavy chain, and cardiotrophin-1 genes (24). Consistent with our results, decreased Erk and Jnk activities were observed in a rat model of heart failure and hypertension (19). Constitutive activation of Mek5, the upstream kinase that activates Erk5, induced cardiomyocyte elongation, leading to dilated cardiomyopathy and sudden death in mice (33). The transcription factor MEF2C has been shown to regulate postnatal heart development and to control gene expression associated with heart hypertrophy. Thus, the Erk5/MEF2C pathway is clearly an important component in cardiac hypertrophy (1).

The development of dilated cardiomyopathy and impairment of cardiac functions in MSKO mice are apparently due to Shp2 deficiency intrinsic to cardiomyocytes, since a recent study showed that mice with deletion of the Shp2 exon 11 in cardiomyocytes mediated by α-myosin heavy chain Cre exhibited a phenotype similar to that induced by Mck-Cre (22). In comparing our results to those of Kontaridis et al. (22), it is interesting that mice with Mck-Cre-mediated exon 4 or exon 11 deletion of *Ptpn11*/*Shp2* showed similar and consistent defects in dilated cardiomyopathy, although with notable differences in severity. The most striking difference is that deletion of exon 4 leads to early mortality in mice, whereas animals with exon 11 ablation have normal life spans. Multiple factors can contribute to this discrepancy, such as genetic background and Cre-mediated DNA recombination efficiency, etc. In addition, the consequence of exon 11 deletion is unclear, and it remains to be clarified whether the removal of exon 11 creates a null allele or a hypomorphic allele producing a C-terminal truncated Shp2 protein.

Associations between cardiomyopathy, insulin resistance, and alterations in glucose uptake have been previously reported in human subjects (35). The molecular basis for this link is unclear, which is largely due to the lack of proper animal models for this complex disease. The most interesting phenotype of MSKO mice is the development of insulin resistance in connection with the cardiac dysfunction phenotype. Both cardiac and skeletal muscle cells in MSKO are defective in insulin-induced glucose uptake. We believe that although Shp2 deficiency can play a direct causative role in dilated cardiomyopathy, the development of insulin resistance may aggravate the progression of heart failure in MSKO mice. In examining metabolic parameters, we found that MSKO mice displayed hyperglyceridemia, an important symptom of metabolic syndromes. This phenotype is very similar to that of muscle-specific insulin receptor knockout (MIRKO) mice, excluding the appearance of dilated cardiomyopathy (3). MIRKO mice exhibit hypertriglyceridemia and impaired glucose uptake in muscle. Although MIRKO mice show a high level of insulin resistance in isolated muscle, it seems insufficient to trigger whole-body insulin resistance (3).

It is well known that Shp2 tyrosine phosphatase acts to modulate the signal strength of multiple pathways, and therefore Shp2 ablation apparently disturbs numerous signaling cascades. In previous experiments, we and others demonstrated that Shp2 physically associates with IRS-1 in insulin-stimulated cells (23). By docking on two phospho-tyrosyl residues (pY1172 and pY1222) at the C-terminal tail (6, 40), Shp2 can dephosphorylate the other phospho-tyrosine sites, such as those for association with the p85 subunit of the PI3K (31). Thus, mutating the two Shp2 docking sites leads to increased tyrosine phosphorylation of IRS-1 and enhanced IRS-1/p85 binding (31). Consistently, we detected stronger pY-IRS-1 signals and increased IRS-1/p85 binding in Shp2-deficient muscle cells. These biochemical data, which suggest a negative role of Shp2 in modulating insulin signaling through IRS-1, are at odds with the insulin resistance phenotype observed in MSKO mice. The modest level of persistent hyperinsulinemia in MSKO mice could contribute in part to development of insulin resistance despite increased pY-IRS-1 signals. Furthermore, disturbance of other downstream signaling pathways can offset the effect of increased IRS-1 signaling and trigger insulin resistance.

Insulin stimulates plasma translocation of glucose transporters and consequently glucose uptake through multiple signaling pathways, involving Akt and atypical PKC (PKC-ζ/λ) (15, 39). Akt activation appears preserved in MSKO mice after insulin stimulation, while phosphorylation of PKC-ζ/λ is decreased in striated muscles isolated from MSKO mice. A previous report has demonstrated that chronic heart failure patients also have impaired insulin-stimulated glucose uptake,

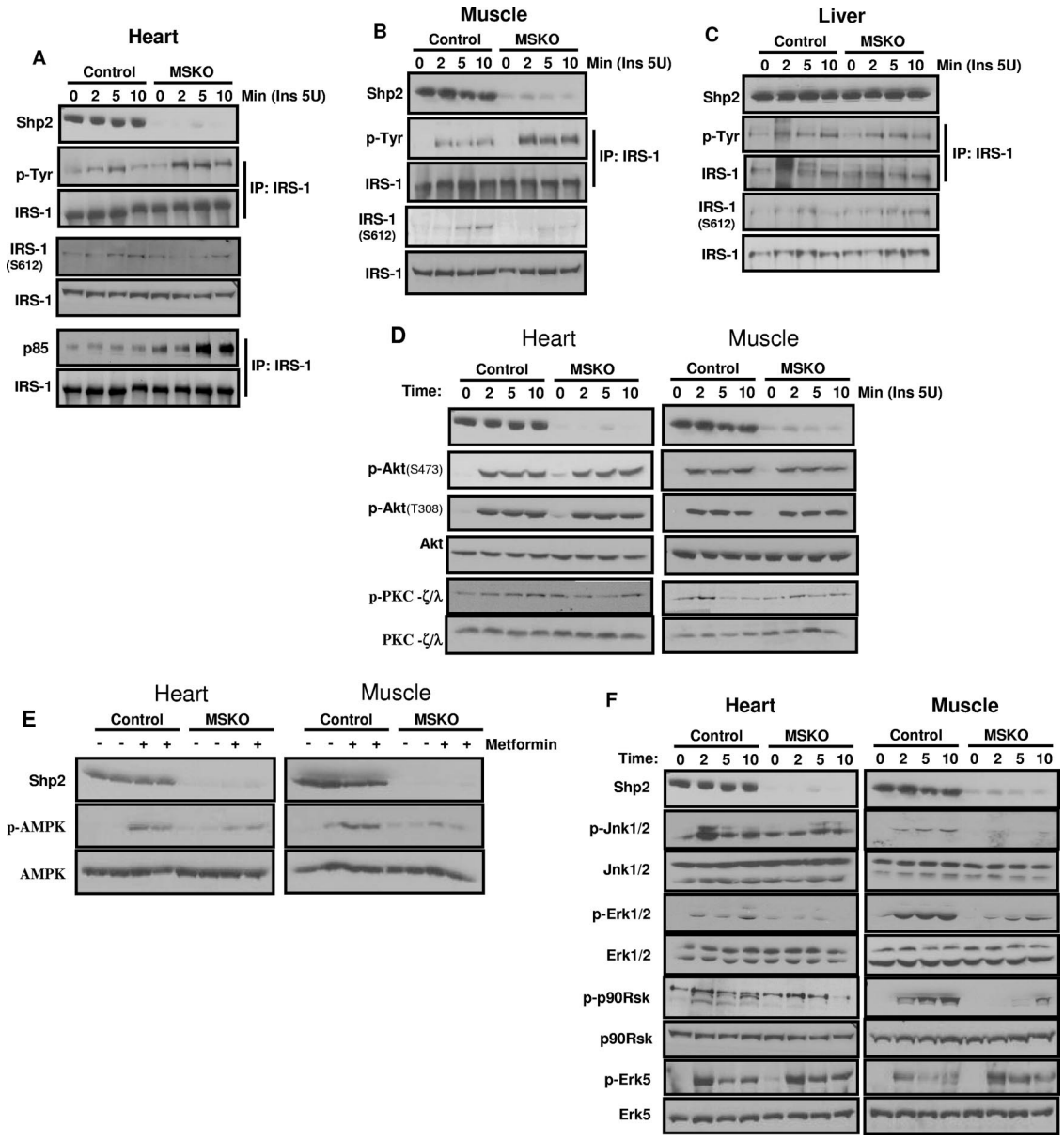

FIG. 7. Insulin-stimulated signaling events. (A to C) Insulin (5 U) was injected into the cava vein, and extracts of heart (A), muscle (B), or liver (C) were subjected to immunoprecipitation or immunoblotting analysis with antibodies as indicated. (D) Tissue samples were collected as in panel A, and immunoblot analyses were done with the indicated antibodies. (E) Metformin (0.4 g/kg) was injected in the cava vein for 5 min. Extracts of heart and muscle were blotted with antibodies as indicated. (F) Insulin (5 U) was injected into the cava veins of overnight fasted mice. Heart and muscle extracts were blotted with antibodies as indicated. The data shown are representative of at least three independent experiments.

despite a normal level of Akt activity in skeletal muscle (20). A mechanism partially dependent on ATP utilization leading to an increased 5′-AMP level and activation of AMPK has been identified to regulate glucose transporter activity and muscle glucose uptake (13, 30). We demonstrated here that AMPK activation after metformin treatment was impaired in MSKO mice. Therefore, selective deletion of Shp2 in striated muscle affected both insulin- and non-insulin-dependent pathways responsible for glucose uptake. The positive effect of Shp2 in mediating insulin-stimulated metabolic responses is consistent with a previous study showing that transgenic expression of a truncated protein containing the SH2 domains of Shp2 induced insulin resistance in mice (26). This is in contrast to a negative role of its close relative Shp1 in the modulation of insulin signal strength (10).

Shp2 deficiency leads to decreased activation of Erk1/2 and Jnk1/2 kinases by insulin but increased activity of Erk5 after insulin stimulation. Thus, aberrant Erk1/2, Jnk1/2, and Erk5 activities apparently contribute to the metabolically defective phenotype of MSKO mice. However, we wanted to reiterate the point that deletion of Shp2 in striated muscle disturbed multiple signaling pathways directly or indirectly, resulting in the development of complex cardiac and metabolic disorders in this mouse model. Heart failure has been identified as a

most common cause of mortality in diabetic patients, and insulin resistance is also a major risk factor in cardiovascular diseases. It is conceivable that the development and progression of a compound disease affecting several organs and tissues could be caused by the accumulation of multiple defects, and indeed experimental and clinical data suggest the involvement of many genes in the etiology of metabolic disorders. Notably, a defect in *Ptpn11*/*Shp2* can also trigger a complex disease, as the gene product acts to regulate multiple pathways. Thus, the MSKO mouse will be a valuable model for the elucidation of molecular links between cardiovascular and metabolic diseases.

ACKNOWLEDGMENTS

This study was supported by NIH grants R01DK73945 to G.-S.F., R01HL082902 to J.C., and R01HL059502 to M.M. R.D.T. is a recipient of a postdoctoral fellowship from American Heart Association. F.S. is a recipient of the AHA National Scientist Development Grant.

REFERENCES

1. **Akazawa, H., and I. Komuro.** 2003. Roles of cardiac transcription factors in cardiac hypertrophy. Circ. Res. **92:**1079–1088.
2. **Bard-Chapeau, E. A., J. Yuan, N. Droin, S. Long, E. E. Zhang, T. V. Nguyen, and G. S. Feng.** 2006. Concerted functions of Gab1 and Shp2 in liver regeneration and hepatoprotection. Mol. Cell. Biol. **26:**4664–4674.
3. **Bruning, J. C., M. D. Michael, J. N. Winnay, T. Hayashi, D. Horsch, D. Accili, L. J. Goodyear, and C. R. Kahn.** 1998. A muscle-specific insulin receptor knockout exhibits features of the metabolic syndrome of NIDDM without altering glucose tolerance. Mol. Cell **2:**559–569.
4. **Camper-Kirby, D., S. Welch, A. Walker, I. Shiraishi, K. D. Setchell, E. Schaefer, J. Kajstura, P. Anversa, and M. A. Sussman.** 2001. Myocardial Akt activation and gender: increased nuclear activity in females versus males. Circ. Res. **88:**1020–1027.
5. **Carroll, R., A. N. Carley, J. R. Dyck, and D. L. Severson.** 2005. Metabolic effects of insulin on cardiomyocytes from control and diabetic db/db mouse hearts. Am. J. Physiol. Endocrinol. Metab. **288:**E900–E906.
6. **Case, R. D., E. Piccione, G. Wolf, A. M. Benett, R. J. Lechleider, B. G. Neel, and S. E. Shoelson.** 1994. SH-PTP2/Syp SH2 domain binding specificity is defined by direct interactions with platelet-derived growth factor beta-receptor, epidermal growth factor receptor, and insulin receptor substrate-1-derived phosphopeptides. J. Biol. Chem. **269:**10467–10474.
7. **Chien, K. R., K. U. Knowlton, H. Zhu, and S. Chien.** 1991. Regulation of cardiac gene expression during myocardial growth and hypertrophy: molecular studies of an adaptive physiologic response. FASEB J. **5:**3037–3046.
8. **Crackower, M. A., G. Y. Oudit, I. Kozieradzki, R. Sarao, H. Sun, T. Sasaki, E. Hirsch, A. Suzuki, T. Shioi, J. Irie-Sasaki, R. Sah, H. Y. Cheng, V. O. Rybin, G. Lembo, L. Fratta, A. J. Oliveira-dos-Santos, J. L. Benovic, C. R. Kahn, S. Izumo, S. F. Steinberg, M. P. Wymann, P. H. Backx, and J. M. Penninger.** 2002. Regulation of myocardial contractility and cell size by distinct PI3K-PTEN signaling pathways. Cell **110:**737–749.
9. **Donthi, R. V., G. Ye, C. Wu, D. A. McClain, A. J. Lange, and P. N. Epstein.** 2004. Cardiac expression of kinase-deficient 6-phosphofructo-2-kinase/fructose-2,6-bisphosphatase inhibits glycolysis, promotes hypertrophy, impairs myocyte function, and reduces insulin sensitivity. J. Biol. Chem. **279:**48085–48090.
10. **Dubois, M. J., S. Bergeron, H. J. Kim, L. Dombrowski, M. Perreault, B. Fournes, R. Faure, M. Olivier, N. Beauchemin, G. I. Shulman, K. A. Siminovitch, J. K. Kim, and A. Marette.** 2006. The SHP-1 protein tyrosine phosphatase negatively modulates glucose homeostasis. Nat. Med. **12:**549–556.
11. **Graveleau, C., V. G. Zaha, A. Mohajer, R. R. Banerjee, N. Dudley-Rucker, C. M. Steppan, M. W. Rajala, P. E. Scherer, R. S. Ahima, M. A. Lazar, and E. D. Abel.** 2005. Mouse and human resistins impair glucose transport in primary mouse cardiomyocytes, and oligomerization is required for this biological action. J. Biol. Chem. **280:**31679–31685.
12. **Hagiwara, Y., S. Miyoshi, K. Fukuda, N. Nishiyama, Y. Ikegami, K. Tanimoto, M. Murata, E. Takahashi, K. Shimoda, T. Hirano, H. Mitamura, and S. Ogawa.** 2007. SHP2-mediated signaling cascade through gp130 is essential for LIF-dependent I CaL, $[Ca^{2+}]_i$ transient, and APD increase in cardiomyocytes. J. Mol. Cell Cardiol. **43:**710–716.
13. **Hardie, D. G.** 2004. AMP-activated protein kinase: the guardian of cardiac energy status. J. Clin. Investig. **114:**465–468.
14. **Hawley, S. A., A. E. Gadalla, G. S. Olsen, and D. G. Hardie.** 2002. The antidiabetic drug metformin activates the AMP-activated protein kinase cascade via an adenine nucleotide-independent mechanism. Diabetes **51:**2420–2425.
15. **Hernandez, R., T. Teruel, and M. Lorenzo.** 2001. Akt mediates insulin induction of glucose uptake and upregulation of GLUT4 gene expression in brown adipocytes. FEBS Lett. **494:**225–231.
16. **Hirota, H., J. Chen, U. A. Betz, K. Rajewsky, Y. Gu, J. Ross, Jr., W. Muller, and K. R. Chien.** 1999. Loss of a gp130 cardiac muscle cell survival pathway is a critical event in the onset of heart failure during biomechanical stress. Cell **97:**189–198.
17. **Johnatty, S. E., J. R. Dyck, L. H. Michael, E. N. Olson, and M. Abdellatif.** 2000. Identification of genes regulated during mechanical load-induced cardiac hypertrophy. J. Mol. Cell Cardiol. **32:**805–815.
18. **Jougasaki, M., H. Leskinen, A. M. Larsen, A. Cataliotti, H. H. Chen, and J. C. Burnett, Jr.** 2003. Leukemia inhibitory factor is augmented in the heart in experimental heart failure. Eur. J. Heart Fail. **5:**137–145.
19. **Kacimi, R., and A. M. Gerdes.** 2003. Alterations in G protein and MAP kinase signaling pathways during cardiac remodeling in hypertension and heart failure. Hypertension **41:**968–977.
20. **Kemppainen, J., H. Tsuchida, K. Stolen, H. Karlsson, M. Bjornholm, O. J. Heinonen, P. Nuutila, A. Krook, J. Knuuti, and J. R. Zierath.** 2003. Insulin signalling and resistance in patients with chronic heart failure. J. Physiol. **550:**305–315.
21. **Kontaridis, M. I., K. D. Swanson, F. S. David, D. Barford, and B. G. Neel.** 2006. PTPN11 (Shp2) mutations in LEOPARD syndrome have dominant negative, not activating, effects. J. Biol. Chem. **281:**6785–6792.
22. **Kontaridis, M. I., W. Yang, K. K. Bence, D. Cullen, B. Wang, N. Bodyak, Q. Ke, A. Hinek, P. M. Kang, R. Liao, and B. G. Neel.** 2008. Deletion of Ptpn11 (Shp2) in cardiomyocytes causes dilated cardiomyopathy via effects on the extracellular signal-regulated kinase/mitogen-activated protein kinase and RhoA signaling pathways. Circulation **117:**1423–1435.
23. **Kuhne, M. R., T. Pawson, G. E. Lienhard, and G. S. Feng.** 1993. The insulin receptor substrate 1 associates with the SH2-containing phosphotyrosine phosphatase Syp. J. Biol. Chem. **268:**11479–11481.
24. **Kunisada, K., S. Negoro, E. Tone, M. Funamoto, T. Osugi, S. Yamada, M. Okabe, T. Kishimoto, and K. Yamauchi-Takihara.** 2000. Signal transducer and activator of transcription 3 in the heart transduces not only a hypertrophic signal but a protective signal against doxorubicin-induced cardiomyopathy. Proc. Natl. Acad. Sci. USA **97:**315–319.
25. **Lai, L. A., C. Zhao, E. E. Zhang, and G. S. Feng.** 2004. The Shp-2 tyrosine phosphatase, p. 275–299. *In* J. Arino and D. Alexander (ed.), Protein phosphatases, vol. 5. Springer-Verlag, Berlin, Germany.
26. **Maegawa, H., M. Hasegawa, S. Sugai, T. Obata, S. Ugi, K. Morino, K. Egawa, T. Fujita, T. Sakamoto, Y. Nishio, H. Kojima, M. Haneda, H. Yasuda, R. Kikkawa, and A. Kashiwagi.** 1999. Expression of a dominant-negative SHP-2 in transgenic mice induces insulin resistance. J. Biol. Chem. **274:**30236–30243.
27. **Matsui, T., L. Li, J. C. Wu, S. A. Cook, T. Nagoshi, M. H. Picard, R. Liao, and A. Rosenzweig.** 2002. Phenotypic spectrum caused by transgenic overexpression of activated Akt in the heart. J. Biol. Chem. **277:**22896–22901.
28. **Milarski, K. L., and A. R. Saltiel.** 1994. Expression of catalytically inactive Syp phosphatase in 3T3 cells blocks stimulation of mitogen-activated protein kinase by insulin. J. Biol. Chem. **269:**21239–21243.
29. **Minamisawa, S., Y. Sato, and M. C. Cho.** 2004. Calcium cycling proteins in heart failure, cardiomyopathy and arrhythmias. Exp. Mol. Med. **36:**193–203.
30. **Musi, N., N. Fujii, M. F. Hirshman, I. Ekberg, S. Froberg, O. Ljungqvist, A. Thorell, and L. J. Goodyear.** 2001. AMP-activated protein kinase (AMPK) is activated in muscle of subjects with type 2 diabetes during exercise. Diabetes **50:**921–927.
31. **Myers, M. G., Jr., R. Mendez, P. Shi, J. H. Pierce, R. Rhoads, and M. F. White.** 1998. The COOH-terminal tyrosine phosphorylation sites on IRS-1 bind SHP-2 and negatively regulate insulin signaling. J. Biol. Chem. **273:**26908–26914.
32. **Neel, B. G., H. Gu, and L. Pao.** 2003. The 'Shp'ing news: SH2 domain-containing tyrosine phosphatases in cell signaling. Trends Biochem. Sci. **28:**284–293.
33. **Nicol, R. L., N. Frey, G. Pearson, M. Cobb, J. Richardson, and E. N. Olson.** 2001. Activated MEK5 induces serial assembly of sarcomeres and eccentric cardiac hypertrophy. EMBO J. **20:**2757–2767.
34. **Ozcelik, C., B. Erdmann, B. Pilz, N. Wettschureck, S. Britsch, N. Hubner, K. R. Chien, C. Birchmeier, and A. N. Garratt.** 2002. Conditional mutation of the ErbB2 (HER2) receptor in cardiomyocytes leads to dilated cardiomyopathy. Proc. Natl. Acad. Sci. USA **99:**8880–8885.
35. **Paternostro, G., D. Pagano, T. Gnecchi-Ruscone, R. S. Bonser, and P. G. Camici.** 1999. Insulin resistance in patients with cardiac hypertrophy. Cardiovasc. Res. **42:**246–253.
36. **Saxton, T. M., M. Henkemeyer, S. Gasca, R. Shen, D. J. Rossi, F. Shalaby, G. S. Feng, and T. Pawson.** 1997. Abnormal mesoderm patterning in mouse embryos mutant for the SH2 tyrosine phosphatase Shp-2. EMBO J. **16:**2352–2364.
37. **Shai, S. Y., A. E. Harpf, C. J. Babbitt, M. C. Jordan, M. C. Fishbein, J. Chen, M. Omura, T. A. Leil, K. D. Becker, M. Jiang, D. J. Smith, S. R. Cherry, J. C. Loftus, and R. S. Ross.** 2002. Cardiac myocyte-specific excision of the beta1 integrin gene results in myocardial fibrosis and cardiac failure. Circ. Res. **90:**458–464.

38. **Shioi, T., P. M. Kang, P. S. Douglas, J. Hampe, C. M. Yballe, J. Lawitts, L. C. Cantley, and S. Izumo.** 2000. The conserved phosphoinositide 3-kinase pathway determines heart size in mice. EMBO J. **19:**2537–2548.
39. **Standaert, M. L., G. Bandyopadhyay, L. Perez, D. Price, L. Galloway, A. Poklepovic, M. P. Sajan, V. Cenni, A. Sirri, J. Moscat, A. Toker, and R. V. Farese.** 1999. Insulin activates protein kinases C-zeta and C-lambda by an autophosphorylation-dependent mechanism and stimulates their translocation to GLUT4 vesicles and other membrane fractions in rat adipocytes. J. Biol. Chem. **274:**25308–25316.
40. **Sugimoto, S., T. J. Wandless, S. E. Shoelson, B. G. Neel, and C. T. Walsh.** 1994. Activation of the SH2-containing protein tyrosine phosphatase, SH-PTP2, by phosphotyrosine-containing peptides derived from insulin receptor substrate-1. J. Biol. Chem. **269:**13614–13622.
41. **Tanaka, N., N. Dalton, L. Mao, H. A. Rockman, K. L. Peterson, K. R. Gottshall, J. J. Hunter, K. R. Chien, and J. Ross, Jr.** 1996. Transthoracic echocardiography in models of cardiac disease in the mouse. Circulation **94:**1109–1117.
42. **Tartaglia, M., E. L. Mehler, R. Goldberg, G. Zampino, H. G. Brunner, H. Kremer, I. van Der Burgt, A. H. Crosby, A. Ion, S. Jeffery, K. Kalidas, M. A. Patton, R. S. Kucherlapati, and B. D. Gelb.** 2001. Mutations in PTPN11, encoding the protein tyrosine phosphatase SHP-2, cause Noonan syndrome. Nat. Genet. **29:**465–468.
43. **Wijesekara, N., D. Konrad, M. Eweida, C. Jefferies, N. Liadis, A. Giacca, M. Crackower, A. Suzuki, T. W. Mak, C. R. Kahn, A. Klip, and M. Woo.** 2005. Muscle-specific Pten deletion protects against insulin resistance and diabetes. Mol. Cell. Biol. **25:**1135–1145.
44. **Wilkes, J. J., A. Hevener, and J. Olefsky.** 2003. Chronic endothelin-1 treatment leads to insulin resistance in vivo. Diabetes **52:**1904–1909.
45. **Witteles, R. M., W. H. Tang, A. H. Jamali, J. W. Chu, G. M. Reaven, and M. B. Fowler.** 2004. Insulin resistance in idiopathic dilated cardiomyopathy: a possible etiologic link. J. Am. Coll. Cardiol. **44:**78–81.
46. **Zhang, E. E., E. Chapeau, K. Hagihara, and G. S. Feng.** 2004. Neuronal Shp2 tyrosine phosphatase controls energy balance and metabolism. Proc. Natl. Acad. Sci. USA **101:**16064–16069.
47. **Zhou, G., R. Myers, Y. Li, Y. Chen, X. Shen, J. Fenyk-Melody, M. Wu, J. Ventre, T. Doebber, N. Fujii, N. Musi, M. F. Hirshman, L. J. Goodyear, and D. E. Moller.** 2001. Role of AMP-activated protein kinase in mechanism of metformin action. J. Clin. Investig. **108:**1167–1174.
48. **Zisman, A., O. D. Peroni, E. D. Abel, M. D. Michael, F. Mauvais-Jarvis, B. B. Lowell, J. F. Wojtaszewski, M. F. Hirshman, A. Virkamaki, L. J. Goodyear, C. R. Kahn, and B. B. Kahn.** 2000. Targeted disruption of the glucose transporter 4 selectively in muscle causes insulin resistance and glucose intolerance. Nat. Med. **6:**924–928.